

Simultaneously Improving the Optical, Dielectric, and Solubility Properties of Fluorene-Based Polyimide with Silyl Ether Side Groups

Yancheng Wu,* Shumei Liu, and Jianqing Zhao

Cite This: *ACS Omega* 2022, 7, 11939–11945

Read Online

ACCESS |



Metrics & More

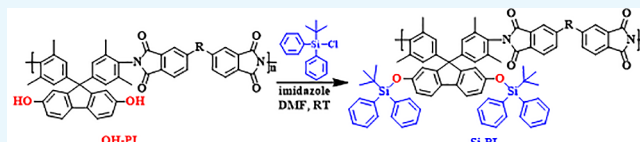


Article Recommendations



Supporting Information

ABSTRACT: Three fluorene-based polyimides with silyl ether groups (Si-PIs) were successfully synthesized by a simple and efficient silicon etherification reaction of hydroxyl-containing polyimides (OH-PIs) and *tert*-butylchlorodiphenylsilane (TBDPSCI), and their structures were confirmed by ¹H NMR and IR spectra. The bulky nonpolar *tert*-butyldiphenylsilyl (TBDPS) side groups in the modified PI unit instead of the strong electron donor –OH group is conducive to decreasing electronic conjugation and charge transfer (CT) interaction along the PI chain. Accordingly, the optical, dielectric, and solubility properties of the modified Si-PI films are simultaneously improved compared with the precursor OH-PI films. The modified Si-PI films demonstrate a meaningful enhancement in the transmittances at a wavelength of 400 nm (T_{400}) to 74–81% from 42 to 55% of OH-PI films and the regeneration of fluorescence characteristics. The dielectric constant and loss of Si-PI films are also obviously reduced to 2.63–2.75 and 0.0024–0.0091 at 1 kHz from 4.19 to 4.78 and 0.0173–0.0295 of OH-PI films, respectively, due to substituted with the bulky nonpolar TBDPS groups to increase the free volume and hydrophobicity of Si-PI films. The solubility of Si-PIs in low- or nonpolar solvents (such as CHCl₃, CH₂Cl₂, acetone, and toluene) is significantly improved. Furthermore, Si-PI films still maintain relatively good thermal properties with the 5% weight loss temperature ($T_{5\%}$) in the range 470–491 °C under a nitrogen atmosphere and the glass transition temperature (T_g) in the range 245–308 °C.



- ✓ Mild modified reaction conditions
- ✓ 100% conversion
- ✓ Increased optical transparency
- ✓ Regeneration of fluorescence characteristics
- ✓ Decreased dielectric constant and loss
- ✓ Improved solubility in low- or non-polar solvents

1. INTRODUCTION

The rapid development of optical and microelectronic technology has brought enormous demand for highly transparent, light-emitting, and low-dielectric permittivity polymeric materials.^{1–5} Among the polymeric materials, polyimides (PIs) have attracted widely attention because of their outstanding comprehensive properties, including remarkable thermal and chemical stabilities and good mechanical strength.^{6–8} Of course, caused by the strong CT interaction in PI chains, aromatic PI also has its defects, such as poor optical transparency and fluorescence, relatively high dielectric constant and loss value, and low solubility in organic solvents, especially in low- or nonpolar organic solvents.^{9–12} These disadvantages limit the in-depth application of PI in modern optical and microelectronic technology, which is urgent to improve.

The preparation of PI/inorganic hybrid materials is considered as a promising way to overcome some aforementioned deficiencies of PI materials.^{13–15} For instance, the PI–organosilicate hybrid is a competitive modifier to simultaneously improve the dielectric and optical properties.^{16–21} However, PI–organosilicate hybrids still have some disadvantages, such as the complex preparation process, the low miscibility between the PI and silicate components, and the poor solubility in organic solvents. In addition, the preparation of PI backbone containing siloxane moieties is another way to obtain the transparent or low-dielectric-

constant PIs.^{22–25} Nevertheless, it is still a great challenge to keep a suitable balance between optical/dielectric properties and other desirable properties, especially heat resistance.

It was revealed that the noncoplanar fluorene-based Cardo PIs show excellent combined properties with high optical transparency and low-*k* value, without sacrificing the desired thermal stabilities properties.^{26–28} This work focuses on the design and preparation of fluorene-based Cardo polyimides with bulky *tert*-butyldiphenylsilyl (TBDPS) side groups (Si-PIs). The incorporation of fluorene-based Cardo structure into PI backbone gives them desired thermal stabilities, mechanical and photoluminescence properties.^{27–29} And meanwhile, introducing the bulky nonpolar TBDPS groups in fluorene-based PIs side chain is able to simultaneously improve their optical, dielectric and solubility properties.³⁰ However, according to the traditional preparation method, the preparation and purification of the bulky structure of diamine monomer containing TBDPS groups is complicated and not easy to achieve.³⁰ In addition, the probably relatively low

Received: January 4, 2022

Accepted: March 18, 2022

Published: April 1, 2022



Scheme 1. Synthesis Routes of Three Si-PIs

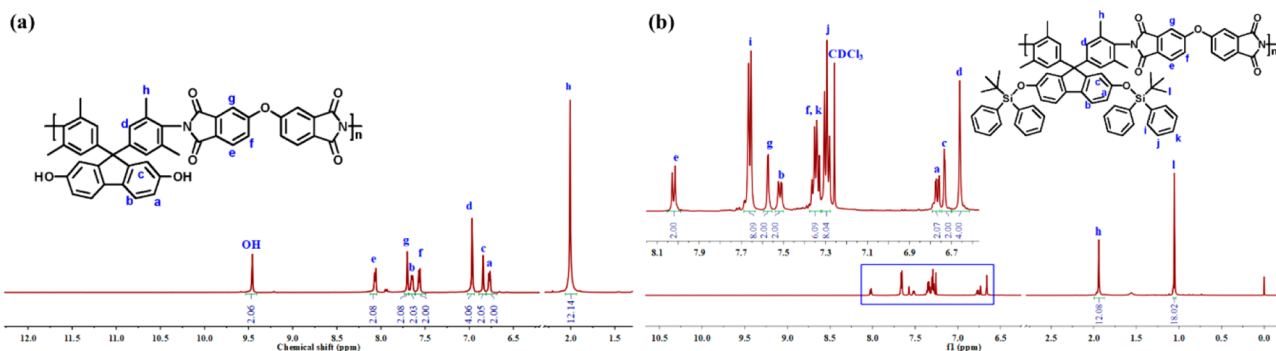
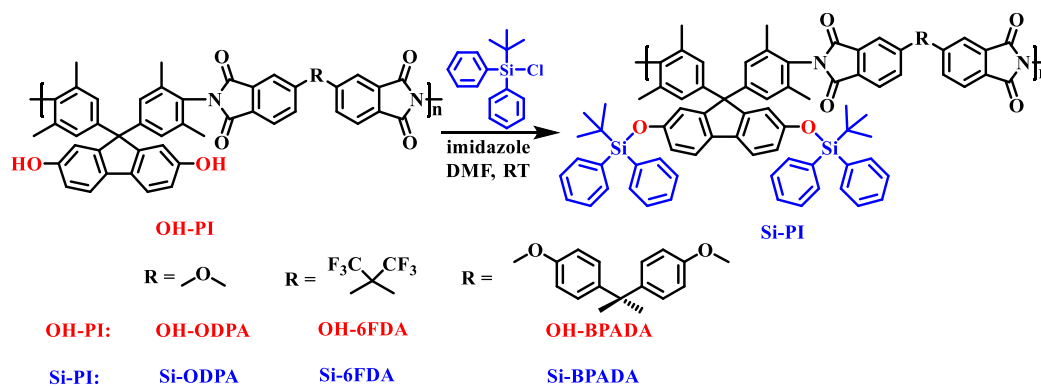


Figure 1. ^1H NMR spectra of polyimides (a) OH-ODPA and (b) Si-ODPA.

polymerization reactivity of the bulky structure of diamine monomer containing TBDPS groups is also not conducive to prepare the corresponding PIs with high molecular weight. To address this issue, a simple postmodification strategy is used to prepare Si-PIs in this work (Scheme 1). The effect of replacing electron-donating hydroxyl groups with bulky nonpolar TBDPS groups in fluorene-based PIs side chain on the optical, dielectric and solubility properties of the resulting Si-PI films was studied.

2. RESULTS AND DISCUSSION

2.1. Preparation and Characterization of Si-PIs.

Three modified fluorene-based PIs with silyl ether groups (Si-PIs) were prepared via a simple and efficient silicon etherification reaction of hydroxyl-containing PIs (OH-PIs) and TBDPSCl at room temperature to afford three modified Si-PIs (Scheme 1). The OH-PIs show a weight-average molecular weight (M_w) of $25.2 \times 10^4 \text{ g}\cdot\text{mol}^{-1}$ for OH-ODPA, $17.2 \times 10^4 \text{ g}\cdot\text{mol}^{-1}$ for OH-6FDA, and $14.0 \times 10^4 \text{ g}\cdot\text{mol}^{-1}$ for OH-BPADA with a polydispersity index of 2.46 for OH-ODPA, 1.77 for OH-6FDA, and 1.52 for OH-BPADA measured by GPC. All obtained Si-PIs exhibit a higher M_w of $26.3 \times 10^4 \text{ g}\cdot\text{mol}^{-1}$ for Si-ODPA, $25.6 \times 10^4 \text{ g}\cdot\text{mol}^{-1}$ for Si-6FDA, and $18.0 \times 10^4 \text{ g}\cdot\text{mol}^{-1}$ for Si-BPADA with a polydispersity index of 2.82 for Si-ODPA, 3.12 for Si-6FDA, and 2.13 for Si-BPADA. The correct structures of three modified Si-PIs were proved by ^1H NMR (Figure 1) and IR spectra (Figure 2).

As shown in Figure 1, the ^1H NMR spectra of polyimides Si-ODPA and OH-ODPA for comparison was used as an example to prove the correct structure of three modified Si-PIs. Obviously, there is no apparent peak at around 9.45 ppm attributed to hydroxyl groups (Figure 1a), while the character-

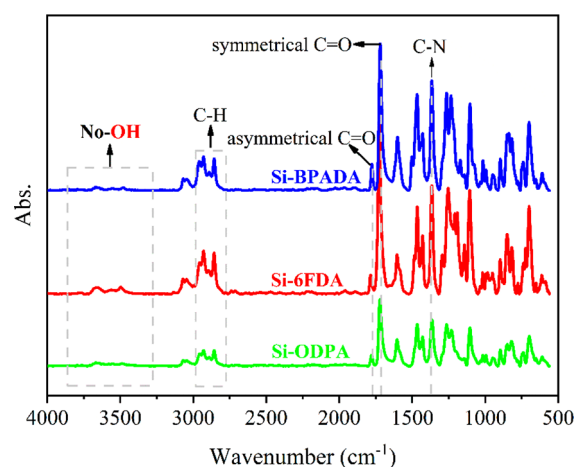


Figure 2. IR spectra of three Si-PI films.

istic single peak of the Si-C(CH₃)₃ (H₁) at 1.05 ppm appears, confirming the introduction of *tert*-butyldiphenylsilyl (TBDPS) groups. At the same time, the ratio of integral areas of the various proton signal peaks in the resulted Si-ODPA chain is perfectly accurate, indicating that TBDPS groups completely supplanted all hydroxyl groups in Si-ODPA chain. Similarly, the correct structure of Si-6FDA (Figure S1 in the Supporting Information) and Si-BPADA (Figure S2 in the Supporting Information) was also determined from their ^1H NMR spectra.

Figure 2 shows the IR spectra of three Si-PI films. The absorption bands at around 1775 cm^{-1} (asymmetrical C=O), 1720 cm^{-1} (symmetrical C=O) and 1365 cm^{-1} (C-N), as well as the absence of hydroxyl absorption peak indicate the successful introduction of TBDPS groups and not the

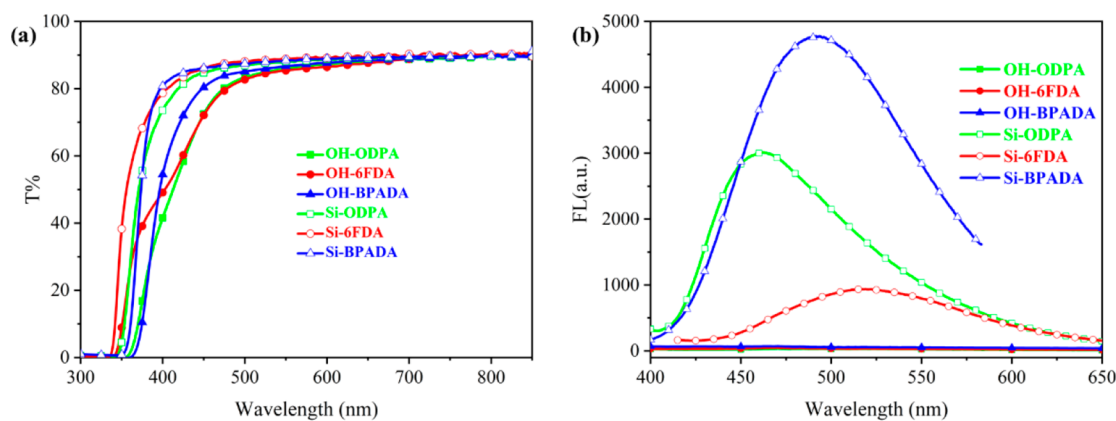


Figure 3. (a) UV-visible transmission and (b) fluorescence spectra of Si-PI and OH-PI films.

Table 1. Optical and Dielectric Properties, Water Absorption, and Contact Angle of PI Films

PIs	λ_0^a (nm)	$T_{400\text{ nm}}^a$ (%)	λ_{em} (nm)	Φ_{PL}^b (%)	T (ns)	k^c	$\tan \delta^c$	W_a^d (%)	WCA ^d (deg)
OH-ODPA	360	42	<i>e</i>	<i>e</i>	<i>e</i>	4.78	0.0173	3.68	75.9
OH-6FDA	343	49	<i>e</i>	<i>e</i>	<i>e</i>	4.19	0.0281	3.11	76.7
OH-BPADA	365	55	<i>e</i>	<i>e</i>	<i>e</i>	4.52	0.0295	1.91	82.8
Si-ODPA	346	74	462	8.5	11.99	2.75	0.0061	0.45	101.0
Si-6FDA	337	79	517	5.2	15.57	2.63	0.0091	0.19	110.3
Si-BPADA	352	81	492	9.3	40.01	2.67	0.0024	0.15	106.4

^aThe thickness of PI films of about 25 μm . ^b Φ_{PL} determined using a calibrated integrating sphere and BaSO₄ as a reference ^cDielectric constant and loss at 1 kHz. ^d W_a : Water absorption. WCA: water contact angle ^eNot detected.

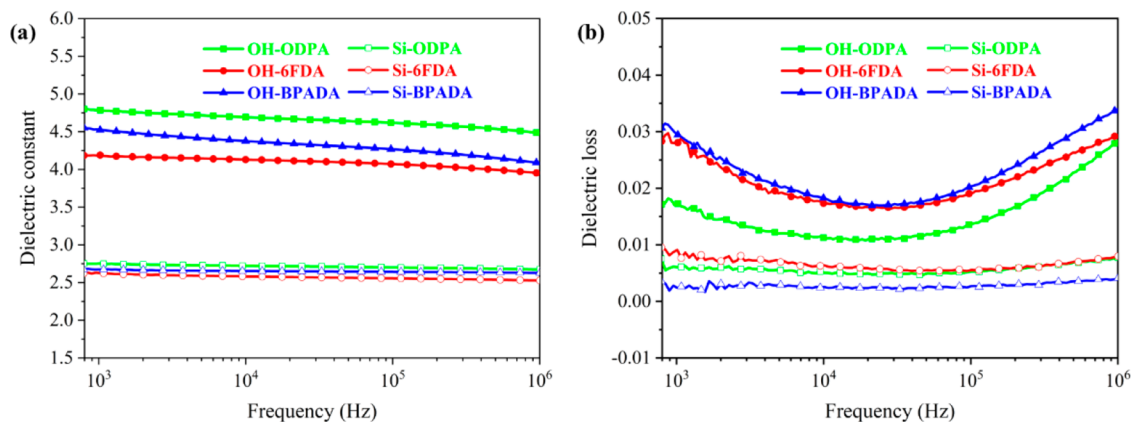


Figure 4. Frequency dependence of the dielectric constant (a) and loss (b) of PI films.

destruction of PI backbone during the silicon etherification. In addition, the absorption band of the symmetrical C=O in the precursor PIs move to a higher wavenumber in the resulted PIs, which further signifies the introduction of TBDPS groups (Figure S3 in the Supporting Information).³¹

2.2. Optical Properties of PI Films. The optical properties of Si-PI films and OH-PI films for comparison were studied by UV-visible and photoluminescence spectroscopic techniques (Figure 3 and Table 1). Apparently, Si-PI films show meaningful enhancement in optical transparency (Figure 3a). The cutoff wavelength (λ_0) is blue-shifted to 337–352 nm for Si-PIs from 343 to 365 nm for OH-PI films (Table 1), and T_{400} of Si-PI films is exceedingly improved to 74–81% from 42 to 55% of OH-PI films. The incorporation of the bulky TBDPS groups instead of the strong electron donor –OH group cut down the electronic conjugation, the packing density and the interchain interactions. Therefore, the

inter- and intrachain CT interaction in Si-PIs chain is suppressed, which is beneficial to improve the optical transparency of Si-PI films.

Despite possessing the fluorene-based fluorescent chromophores in OH-PI chains, OH-PI films show nonfluorescence characteristics. It is because the fluorescence is quenched by the strong CT effect in OH-PI chains (Figure 3b). Conversely, Si-PI films exhibit prominent fluorescent performance with a maximum emission wavelength (λ_{em}) at 462 nm for Si-ODPA, 517 nm for Si-6FDA, and 492 nm for Si-BPADA (Figure 3b and Figure S4 in the Supporting Information), an absolute fluorescence quantum yield (Φ_{PL}) of 8.5% for Si-ODPA, 2.5% for Si-6FDA, and 9.3% for Si-BPADA (Table 1) and a photoluminescence lifetime (τ) of 12.0 ns for Si-ODPA, 15.6 ns for Si-6FDA and 40.0 ns for Si-BPADA (Figure S5 in the Supporting Information and Table 1). The introduction of TBDPS groups in PI side chains

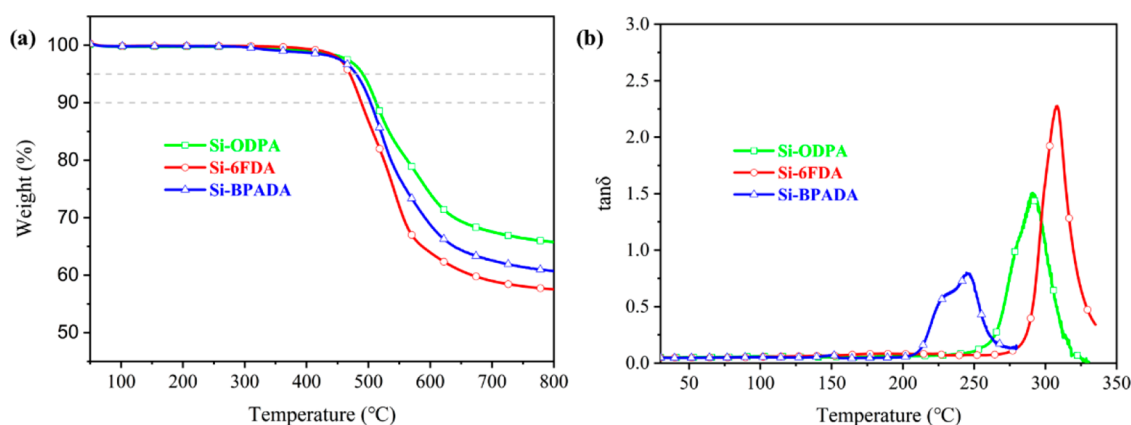


Figure 5. (a) TGA and (b) the loss tangent-temperature curves of PI-TBS films.

is especially important in the regeneration of fluorescent performance in Si-PI films, because it changes the electronic structure along the Si-PI backbone by turning an electron donor (OH) into a bulky group (TBDPS).³² The significant emission intensity of three modified Si-PIs makes them suitable candidates for optical devices and film-based fluorescent sensors for the selective detection of fluoride ion.³³

2.3. Dielectric Properties of PI Films. Dielectric constant (k) and dielectric loss ($\tan \delta$) are vital parameters for applying polymer films in microelectronic devices. The frequency-dependent dielectric properties of OH-PI and Si-PI films are studied at room temperature (Figure 4), and their k and dielectric loss values at 1 kHz are outlined in Table 1. With the introduction of TBDPS groups, the k values of the modified Si-PIs are much reduced than those of the precursor OH-PIs. The k values at 1 kHz of OH-ODPA, OH-6FDA and OH-BPADA are 4.78, 4.19, and 4.52, respectively, while those of Si-ODPA, Si-6FDA and Si-BPADA are as low as 2.75, 2.63, and 2.67, respectively. Moreover, the $\tan \delta$ values of the modified Si-PIs are also dramatically decreased to 0.0024–0.0091 from 0.0173 to 0.0295 of the precursor OH-PIs. It can be observed that the dielectric properties of Si-PI films show higher frequency stability than those of OH-PI films, and their dielectric constants and loss hardly change in the frequency range. The increased free volume and lower polarizability of the modified Si-PIs obtained by turning the polar OH groups into the bulky nonpolar TBDPS groups might be the main reason for the decrease in the dielectric constant and loss of Si-PI films, respectively.^{34,35} Besides, with the introduction of TBDPS groups, the hydrophobicity of Si-PI films is much higher than that of OH-PI films (Figure S6 in the Supporting Information and Table 1), which is also conducive to decreasing the dielectric constant.

2.4. Solubility Property. Due to the existence of rigid nonplanar fluorene unit with two polar hydroxyl groups, the precursor OH-PIs show high solubility in polar solvents such as DMF, DMAc, NMP, *m*-cresol, dioxane, and THF. However, the precursor OH-PIs show relatively poor solubility in low- or nonpolar solvents, such as CHCl₃, CH₂Cl₂, acetone, and toluene (Table S1 in the Supporting Information). With the introduction of bulky nonpolar TBDPS groups to lower the interchain interactions, the modified Si-PIs not only maintain a high solubility in polar solvents except for DMSO, but also show an improved solubility in nonpolar solvents (Table S1 in the Supporting Information). Among three modified SI-PIs, the Si-6FDA shows the best solubility due to the

incorporation of bulky $-(CF_3)_2-$ groups in the PI backbone, which is able to dissolve in acetone at room temperature. Since low- or nonpolar solvents have low boiling temperatures, the good solubility of the modified SI-PIs in these solvents is conducive to formation of PI films or coatings at room temperature, which is very important in terms of material processability.³⁶

2.5. Thermal Properties of PI Films. The thermal properties of Si-PI films are investigated by TGA measurement (Figure 5a) and DMA (Figure 5b), and the results are listed in Table 2. Three modified Si-PI films display good

Table 2. Thermal Properties of PI Films

PIs	$T_{d5\%}^a$ (°C)	$T_{d10\%}^a$ (°C)	R_w^b (%)	T_g^c (°C)
OH-ODPA ^d	527	559	67.1	444
OH-6FDA ^d	516	537	66.0	441
OH-BPADA ^d	501	522	66.2	365
Si-ODPA	491	513	65.7	292
Si-6FDA	470	489	57.2	308
Si-BPADA	480	504	60.7	245

^aThe 5% and 10% weight loss temperatures measured by TGA.

^bResidual weight percentages at 800 °C under nitrogen flow.

^cMeasured by DMA at 1 Hz and at a rate of 5 °C/min. ^dThe data of thermal properties of the precursor OH-PI films come from our previous literatures.^{31,37}

thermal stability with a barely noticeable loss stage up to 400 °C (Figure 5a). The decomposition temperatures at 5% and 10% weight loss ($T_{d5\%}$ and $T_{d10\%}$, respectively) of Si-PI films are in the ranges 470–491 and 489–513 °C, respectively (Table 2). In addition, the char yield at 800 °C of Si-PI films is more than 57.2% (Table 2).

The glass transition temperatures (T_g) of Si-PI films are determined by the peaks at the loss tangent-temperature curves (Figure 5b). After introducing TBDPS groups, the T_g values decrease as expected. However, three modified Si-PI films still maintain relatively high T_g values (245–308 °C, Table 2). Among three modified Si-PI films, the T_g value of Si-6FAD is the highest (308 °C, Table 2), which is correlated to the rigidity of the dianhydride moieties.

After the above discussion, it is evident that the modified Si-PI films display lower thermal stability compared with OH-PI films,^{31,37} which can be explained by the reduced intermolecular attraction forces (e.g., hydrogen bonding) in Si-PI chain and the increased free volume associated with the

TBDPS groups. However, these modified Si-PI films still possess comparatively high thermal stabilities, as well as high transparency and fluorescence, low k , and high solubility in both polar and nonpolar solvents, which are much better than those of the aromatic PI containing bulky side groups reported in the literature.^{38–42} The multifunctional Si-PI films with excellent combined properties are suitable for wide applications in optical and microelectronic devices.

3. CONCLUSIONS

In summary, we have developed a convenient postmodification strategy to synthesize the fluorene-based PIs with silyl ether groups (Si-PIs) by the direct structural modification of the precursor PIs with hydroxyl groups (OH-PIs). With the introduction of TBDPS groups to decrease the interchain interactions, the modified Si-PIs show the excellently increased optical transparency (74–81% at 400 nm), the regeneration of fluorescence characteristics, the decreased dielectric constant and loss (2.63–2.75 and 0.0024–0.0091 at 1 kHz, respectively), and the improved solubility in low- or nonpolar solvents. Meanwhile, the modified Si-PIs still maintain comparatively high thermal stabilities ($T_{5\%} > 470$ °C under a nitrogen atmosphere and $T_g > 245$ °C). This work offers a simple method for preparing multifunctional PI films with outstanding comprehensive properties, giving them potential applications in the areas of optical and microelectronic devices, fluorescent film-based sensors, and so on.

4. EXPERIMENTAL SECTION

4.1. Materials and Methods. Three precursor fluorene-based Cardo PIs with hydroxyl groups (namely OH-PIs) were prepared according to our previous literatures.^{31,37} *tert*-Butylchlorodiphenylsilane (TBDPSCI) and imidazole were purchased from Energy Chemical Co., Ltd. All solvents were purchased from Guangzhou Chemical Reagent Co., Ltd., and used without purification.

Weight-average molecular weight (M_n) and polydispersity index (\bar{D}) of OH-PIs and Si-PIs were estimated by GPC (Waters 1515 pump, Torrance, CA) with DMF and chloroform as the solvent, respectively, and using polystyrene as the reference. ^1H NMR spectra were obtained on a DRX-400 spectrometer or a DRX-600 spectrometer in a solution of DMSO- d_6 for OH-ODPA, and CDCl_3 for Si-PIs with TMS as an internal standard. FT-IR spectra of the studied PI films were performed on a Bruker Vector-22 spectrometer. UV-vis transmission spectra of the studied PI films were performed on an UV-3900 spectrometer (Hitachi, Japan). Fluorescence spectra of the studied PI films were recorded using a Hitachi F-4500 FL spectrophotometer. The fluorescence spectra were obtained with excitation at the peak wavelength of the corresponding excitation spectra. The fluorescence lifetime (τ) of the modified Si-PI films was measured using a Hamamatsu C11367-11 Quantaaurus-Tau time-resolved spectrometer. The fluorescence quantum yield (Φ_{PL}) of the modified Si-PI films was determined on a Hamamatsu absolute PL quantum yield spectrometer C11347 Quantaaurus_QY. Samples were excited at the wavelength of corresponding excitation peak. The dielectric constant (k) was calculated from the following equation: $k = Cd/Sk_0$, where C is the capacitance, d is the thickness of the film, S is the effective area of the film coated by electrodes, and k_0 is the vacuum permittivity (8.854 pF/m). An ALCR meter (4284A,

Agilent) equipped with a dielectric kit (16451B, Agilent) was used to measure the capacitance of the studied PI film at a frequency from 1 to 10^6 Hz. Thermal stability of the modified Si-PI films was performed on a NETZSCH thermogravimetric analyzer (TGA 209F1) from 50 to 800 °C under nitrogen at a heating rate of 10 °C/min. The glass transition temperature (T_g) of the modified Si-PI films was obtained from the temperature corresponding to maximum dynamic mechanical loss tangent ($\tan \delta$) on a NETZSCH dynamic mechanical analyzer (DMA 242C) in tensile mode at a preload force of 0.01 N, an amplitude of 15 μm , and a frequency of 1 Hz at a heating rate of 5 °C.

4.2. Synthesis of Fluorene-Based Cardo PIs with Silyl Ether Groups (Si-PIs). The synthesis of polyimide Si-ODPA was used as an example to illustrate the general synthetic procedure of the modified fluorene-based Cardo PIs with silyl ether groups (Si-PIs). A round-bottom flask was charged with OH-ODPA (1.577 g; 2 mmol) TBDPSCI (0.904 g; 6 mmol) and imidazole (0.408 g; 6 mmol) in 15 mL DMF. The reaction mixture was stirred at room temperature under N_2 for 24 h. After reaction, the homogeneous solution was slowly poured into stirred ethanol (500 mL) to afford a fibrous precipitate, which was washed thoroughly with ethanol and dried in a vacuum oven at 100 °C. At last, the crude polymer precipitate was reprecipitated with CHCl_3 -ethanol to give a pure polymer precipitate. To obtain the PI film, the resulting polymer precipitate was dissolved in DMAc (the solid content of 10 wt %) to afford a homogeneous solution, which was casted onto a clean glass plate and then dried in vacuum for 3 h at 70 °C and for additional 3 h at 200 °C. The PI film was peeled off automatically after the glass plate was immersed in water.

Si-ODPA. Yield: 94.1%. GPC data: $M_w = 25.2 \times 10^4$ g·mol $^{-1}$, $\bar{D} = 2.82$. ^1H NMR (400 MHz, CDCl_3) $\delta = 8.02$ (d, $J = 5.4$ Hz, 2H), 7.66 (d, $J = 4.5$ Hz, 8H), 7.58 (s, 2H), 7.52 (d, $J = 6.8$ Hz, 2H), 7.35 (dd, $J = 9.1, 5.1$ Hz, 6H), 7.29 (t, $J = 4.9$ Hz, 8H), 6.77 (d, $J = 6.8$ Hz, 2H), 6.73 (s, 2H), 6.66 (s, 4H), 1.94 (s, 12H), 1.05 (s, 18H).

Si-6FDA. Yield: 96.3%. GPC data: $M_w = 17.2 \times 10^4$ g·mol $^{-1}$, $\bar{D} = 3.12$. ^1H NMR (600 MHz, CDCl_3) $\delta = 8.06$ (d, $J = 8.0$ Hz, 2H), 7.98 (s, 2H), 7.91 (d, $J = 7.3$ Hz, 2H), 7.66 (d, $J = 6.9$ Hz, 8H), 7.35 (t, $J = 7.4$ Hz, 6H), 7.29 (t, $J = 7.3$ Hz, 8H), 6.79 (d, $J = 8.3$ Hz, 2H), 6.73 (s, 2H), 6.65 (s, 4H), 1.94 (s, 12H), 1.05 (s, 18H).

Si-BPADA. Yield: 94.7%. GPC data: $M_w = 14.0 \times 10^4$ g·mol $^{-1}$, $\bar{D} = 2.13$. ^1H NMR (600 MHz, CDCl_3) $\delta = 7.89$ (d, $J = 8.2$ Hz, 2H), 7.66 (d, $J = 6.9$ Hz, 8H), 7.43 (d, $J = 1.9$ Hz, 2H), 7.38–7.27 (m, 20H), 7.05 (d, $J = 8.6$ Hz, 4H), 6.81–6.71 (m, 4H), 6.65 (s, 4H), 1.91 (s, 12H), 1.76 (s, 6H), 1.06 (s, 18H).

■ ASSOCIATED CONTENT

Supporting Information

The Supporting Information is available free of charge at <https://pubs.acs.org/doi/10.1021/acsomega.2c00069>.

^1H NMR spectra of Si-6FDA and Si-BPADA, partial FT-IR spectra of OH-PI and Si-PI films, photographs of the modified Si-PI films under 365 nm UV light, photoluminescence decay curves at the maximum emission wavelength of Si-PI films, water contact angle values of the modified Si-PI films, and the table of solubility behavior of PIs (PDF)

AUTHOR INFORMATION

Corresponding Author

Yancheng Wu – Guangdong–Hong Kong Joint Laboratory for New Textile Materials, School of Textile Materials and Engineering, Wuyi University, Jiangmen, Guangdong 529020, P. R. China; School of Materials Science and Engineering, South China University of Technology, Guangzhou 510640, P. R. China; orcid.org/0000-0001-5895-8404; Email: yancheng_wu@126.com

Authors

Shumei Liu – School of Materials Science and Engineering, South China University of Technology, Guangzhou 510640, P. R. China; orcid.org/0000-0003-3246-3811

Jianqing Zhao – School of Materials Science and Engineering, South China University of Technology, Guangzhou 510640, P. R. China

Complete contact information is available at:

<https://pubs.acs.org/10.1021/acsomega.2c00069>

Author Contributions

The manuscript was written through contributions of all authors. All authors have given approval to the final version of the manuscript.

Notes

The authors declare no competing financial interest.

ACKNOWLEDGMENTS

We are grateful to the Guangdong Basic and Applied Basic Research Foundation (No. 2020A1515110767), Guangdong Science and Technology Major Special Fund (No. 2019-252), the Science Foundation for Young Research Group of Wuyi University (No. 2020AL016), the Key Basic Research and Applied Basic Research Program of Guangdong Province (No. 2019B1515120073) and the Key 5G Communication Materials and Applications Program of Guangdong Province (No. 2020B010179001).

REFERENCES

- (1) Loste, J.; Lopez-Cuesta, J.-M.; Billon, L.; Garay, H.; Save, M. Transparent polymer nanocomposites: An overview on their synthesis and advanced properties. *Prog. Polym. Sci.* **2019**, *89*, 133–158.
- (2) Wang, H.; Ji, X.; Li, Z.; Huang, F. Fluorescent supramolecular polymeric materials. *Adv. Mater.* **2017**, *29*, 1606117.
- (3) Ji, D.; Li, T.; Hu, W.; Fuchs, H. Recent progress in aromatic polyimide dielectrics for organic electronic devices and circuits. *Adv. Mater.* **2019**, *31*, 1806070.
- (4) Wei, J.; Zhu, L. Intrinsic polymer dielectrics for high energy density and low loss dielectric energy storage. *Prog. Polym. Sci.* **2020**, *106*, 101254.
- (5) Wang, L.; Liu, C.; Shen, S.; Xu, M.; Liu, X. Low dielectric constant polymers for high speed communication network. *Adv. Ind. Eng. Polym. Res.* **2020**, *3*, 138–148.
- (6) Liaw, D.-J.; Wang, K.-L.; Huang, Y.-C.; Lee, K.-R.; Lai, J.-Y.; Ha, C.-S. Advanced polyimide materials: Syntheses, physical properties and applications. *Prog. Polym. Sci.* **2012**, *37*, 907–974.
- (7) Ding, Y.; Hou, H.; Zhao, Y.; Zhu, Z.; Fong, H. Electrospun polyimide nanofibers and their applications. *Prog. Polym. Sci.* **2016**, *61*, 67–103.
- (8) Ma, P.; Dai, C.; Wang, H.; Li, Z.; Liu, H.; Li, W.; Yang, C. A review on high temperature resistant polyimide films: Heterocyclic structures and nanocomposites. *Compos. Commun.* **2019**, *16*, 84–93.
- (9) Hasegawa, M.; Horie, K. Photophysics, photochemistry, and optical properties of polyimides. *Prog. Polym. Sci.* **2001**, *26*, 259–335.
- (10) Yi, L.; Huang, W.; Yan, D. Polyimides with side groups: synthesis and effects of side groups on their properties. *J. Polym. Sci., Part A: Polym. Chem.* **2017**, *55*, 533–559.
- (11) Wang, Y.; Zhou, J.; Chen, X.; Sun, J.; Fang, Q. New colorless and transparent poly(ether imide) derived from a biobased plant oil (Anethole): Synthesis and properties. *ACS Sustainable Chem. Eng.* **2019**, *7*, 11728–11734.
- (12) Yang, Z.; Guo, H.; Kang, C.; Gao, L. Synthesis and characterization of amide-bridged colorless polyimide films with low CTE and high optical performance for flexible OLED displays. *Polym. Chem.* **2021**, *12*, 5364–5376.
- (13) Tsai, C.-L.; Yen, H.-J.; Liou, G.-S. Highly transparent polyimide hybrids for optoelectronic applications. *React. Funct. Polym.* **2016**, *108*, 2–30.
- (14) Yin, X.; Feng, Y.; Zhao, Q.; Li, Y.; Li, S.; Dong, H.; Hu, W.; Feng, W. Highly transparent, strong, and flexible fluorographene/fluorinated polyimide nanocomposite films with low dielectric constant. *J. Mater. Chem. C* **2018**, *6*, 6378–6384.
- (15) Wang, C.-Y.; Chen, W.-T.; Xu, C.; Zhao, X.-Y.; Li, J. Fluorinated polyimide/POSS hybrid polymers with high solubility and low dielectric constant. *Chin. J. Polym. Sci.* **2016**, *34*, 1363–1372.
- (16) Lai, H.; Qin, L.; Liu, X.; Gu, Y. Synthesis of novel polyimides with (tert-butyl dimethylsiloxy)biphenyloxy groups and the effect of side-chains content on their properties. *Eur. Polym. J.* **2008**, *44*, 3724–3731.
- (17) Kivılcım, N.; Seçkin, T.; Köytepe, S. Porous pyridine based polyimide–silica nanocomposites with low dielectric constant. *J. Porous Mater.* **2013**, *20*, 709–718.
- (18) Jung, Y.; Byun, S.; Park, S.; Lee, H. Polyimide-organosilicate hybrids with improved thermal and optical properties. *ACS Appl. Mater. Interfaces* **2014**, *6*, 6054–6061.
- (19) Bae, W. J.; Kovalev, M. K.; Kalinina, F.; Kim, M.; Cho, C. Towards colorless polyimide/silica hybrids for flexible substrates. *Polymer* **2016**, *105*, 124–132.
- (20) Mekuria, T. D.; Chunhong, Z.; Yingnan, L.; El Din Fouad, D.; Lv, K.; Yang, M.; Zhou, Y. Surface modification of nano-silica by diisocyanates and their application in polyimide matrix for enhanced mechanical, thermal and water proof properties. *Mater. Chem. Phys.* **2019**, *225*, 358–364.
- (21) Nam, K.-H.; Jin, J.; Lee, D. H.; Han, H.; Goh, M.; Yu, J.; Ku, B.-C.; You, N.-H. Towards solution-processable, thermally robust, transparent polyimide chain-end tethered organosilicate nanohybrids. *Compos. Part B-Eng.* **2019**, *163*, 290–296.
- (22) Babanzadeh, S.; Mahjoub, A. R.; Mehdipour-Ataei, S. Novel soluble thermally stable silane-containing aromatic polyimides with reduced dielectric constant. *Polym. Degrad. Stab.* **2010**, *95*, 2492–2498.
- (23) Rafiemanzelat, F.; Khoshfetrat, S. M.; Kolahdoozan, M. Fast and eco-friendly synthesis of novel soluble thermally stable poly-(amide-imide)s modified with siloxane linkage with reduced dielectric constant under microwave irradiation in TBAB, TBPB, and MeBuImCl via isocyanate method. *J. Appl. Polym. Sci.* **2013**, *127*, 2371–2379.
- (24) Maegawa, T.; Miyashita, O.; Irie, Y.; Imoto, H.; Naka, K. Synthesis and properties of polyimides containing hexaisobutyl-substituted T8 cages in their main chains. *RSC Adv.* **2016**, *6*, 31751–31757.
- (25) Kaya, I.; Kamaci, M. Poly(azomethine-imide)s containing siloxane moieties: Optical, thermal, mechanical, and morphological properties. *J. Appl. Polym. Sci.* **2020**, *137*, 48364.
- (26) Wang, C.; Chen, W.; Chen, Y.; Zhao, X.; Li, J.; Ren, Q. Synthesis and properties of new fluorene-based polyimides containing trifluoromethyl and isopropyl substituents. *Mater. Chem. Phys.* **2014**, *144*, 553–559.
- (27) Qu, L.; Huang, S.; Zhang, Y.; Chi, Z.; Liu, S.; Chen, X.; Xu, J. Multi-functional polyimides containing tetraphenyl fluorene moieties: fluorescence and resistive switching behaviors. *J. Mater. Chem. C* **2017**, *5*, 6457–6466.

(28) Liu, Y.; Zhou, Z.; Qu, L.; Zou, B.; Chen, Z.; Zhang, Y.; Liu, S.; Chi, Z.; Chen, X.; Xu, J. Exceptionally thermostable and soluble aromatic polyimides with special characteristics: intrinsic ultralow dielectric constant, static random access memory behaviors, transparency and fluorescence. *Mater. Chem. Front.* **2017**, *1*, 326–337.

(29) Liu, Y.-W.; Tang, L.-S.; Qu, L.-J.; Liu, S.-W.; Chi, Z.-G.; Zhang, Y.; Xu, J.-R. Synthesis and properties of high performance functional polyimides containing rigid nonplanar conjugated fluorene moieties. *Chin. J. Polym. Sci.* **2019**, *37*, 416–427.

(30) Lai, H.; Qin, L.; Liu, X.; Gu, Y. Synthesis of novel polyimides with (*tert*-butyldimethylsiloxy)biphenyloxy groups and the effect of side-chains content on their properties. *Eur. Polym. J.* **2008**, *44*, 3724–3731.

(31) Wu, Y.; Ji, J.; Huang, H.; Liu, S.; Zhao, J. Facile synthesis of acyloxy-containing fluorene-based Cardo polyimides with high optical transparency, fluorescence and low dielectric constant. *React. Funct. Polym.* **2021**, *166*, 104979.

(32) Zhou, Z.; Huang, W.; Long, Y.; Chen, Y.; Yu, Q.; Zhang, Y.; Liu, S.; Chi, Z.; Chen, X.; Xu, J. An oxidation-induced fluorescence turn-on approach for non-luminescent flexible polyimide films. *J. Mater. Chem. C* **2017**, *5*, 8545–8552.

(33) Chen, P.; Bai, W.; Bao, Y. Fluorescent chemodosimeters for fluoride ions via silicon-fluorine chemistry: 20 years of progress. *J. Mater. Chem. C* **2019**, *7*, 11731–11746.

(34) Lv, P.; Dong, Z.; Dai, X.; Qiu, X. Flexible polydimethylsiloxane-based porous polyimide films with an ultralow dielectric constant and remarkable water resistance. *ACS Appl. Polym. Mater.* **2019**, *1*, 2597–2605.

(35) Zheng, H.; Wang, C.; Tao, Z.; Jiang, C.; Zhao, X.; Li, J.; Ren, Q. Soluble polyimides containing bulky rigid terphenyl groups with low dielectric constant and high thermal stability. *J. Electron. Mater.* **2021**, *50*, 6981–6990.

(36) Wang, C.-Y.; Jiang, C.-R.; Yu, B.; Zhao, X.-Y.; Cui, Z.-L.; Li, J.; Ren, Q. Highly soluble polyimides containing di-*tert*-butylbenzene and dimethyl groups with good gas separation properties and optical transparency. *Chin. J. Polym. Sci.* **2020**, *38*, 759–768.

(37) Wu, Y.; Shi, C.; Chen, Z.; Zhou, Y.; Liu, S.; Zhao, J. A novel hydroxyl-containing polyimide as a colorimetric and ratiometric chemosensor for the reversible detection of fluoride ions. *Polym. Chem.* **2019**, *10*, 1399–1406.

(38) Wang, C.; Yu, B.; Jiang, C.; Zhao, X.; Li, J.; Ren, Q. Synthesis and characterization of an aromatic diamine and its polyimides containing asymmetric large side groups. *Polym. Bull.* **2020**, *77*, 6509–6523.

(39) Wang, C.; Cao, S.; Chen, W.; Xu, C.; Zhao, X.; Li, J.; Ren, Q. Synthesis and properties of fluorinated polyimides with multi-bulky pendant groups. *RSC Adv.* **2017**, *7*, 26420–26427.

(40) Wang, C.; Yu, B.; Jiang, C.; Zhao, X.; Li, J.; Ren, Q. Synthesis and characterization of an aromatic diamine and its polyimides containing asymmetric large side groups. *Polym. Bull.* **2020**, *77*, 6509–6523.

(41) Tharakan, S. A.; Muthusamy, S. The effects of long and bulky aromatic pendent groups with flexible linkages on the thermal, mechanical and electrical properties of the polyimides and their nanocomposites with functionalized silica. *RSC Adv.* **2021**, *11*, 16645–16660.

(42) Hu, K.; Ye, Q.; Fan, Y.; Nan, J.; Chen, F.; Gao, Y.; Shen, Y. Preparation and characterization of organic soluble polyimides with low dielectric constant containing trifluoromethyl for optoelectronic application. *Eur. Polym. J.* **2021**, *157*, 110566.